IOPscience iopscience.iop.org

Home Search Collections Journals About Contact us My IOPscience

Two-gap, high temperature superconductor, ARPES data, the pseudogap, and magnetic circular dichroism from the negative-*U* perspective

This article has been downloaded from IOPscience. Please scroll down to see the full text article.

2008 J. Phys.: Condens. Matter 20 015205

(http://iopscience.iop.org/0953-8984/20/1/015205)

View the table of contents for this issue, or go to the journal homepage for more

Download details:
IP Address: 129.252.86.83
The article was downloaded on 29/05/2010 at 07:19

Please note that terms and conditions apply.

IOP PUBLISHING JOURNAL OF PHYSICS: CONDENSED MATTER

J. Phys.: Condens. Matter **20** (2008) 015205 (9pp) doi:10.1088/0953-8984/20/01/015205

Two-gap, high temperature superconductor, ARPES data, the pseudogap, and magnetic circular dichroism from the negative-U perspective

John A Wilson

H H Wills Physics Laboratory, University of Bristol, Bristol BS8 1TL, UK

E-mail: john.a.wilson@bris.ac.uk

Received 12 March 2007, in final form 8 November 2007
Published 29 November 2007
Online at stacks.iop.org/JPhysCM/20/015205

Abstract

Recent photoemission work on underdoped high temperature superconductor cuprates between T_c and T^*, the pseudogap temperature, are interpreted within the framework of a previously developed two-subsystem, resonant negative-U scenario. From this exposition, incorporating a developed 2**q** diagonal striping model, detailed understanding follows of the angle resolved photoemission spectroscopy (ARPES) results together with certain scanning tunnelling microscopy and far-infrared optical data. The origin of the magnetic circular dichroism and related effects shown by such materials below T^* is explained.

1. Introduction and background to negative-U interpretation of cuprate HTSC behaviour

A pair of closely related ARPES papers were recently published by Tanaka *et al* [1] and Valla *et al* [2] of immediate relevance to the high temperature superconducting mechanism active in the hole-doped mixed-valent cuprates. Both probe the underdoped side of the phase diagram and the relationship there of the raised temperature pseudogap condition to the low temperature superconductively gapped state. In the underdoped regime these two kinds of DOS gapping, while similar in general angular form (nodes in the 45° basal Brillouin zone diagonals and maxima in the Fermi surface saddle/Cu–O bond directions) have been affirmed as anticorrelated in magnitude. Upon reduction in hole count from optimal doping ($p \approx 0.15$), the superconducting gap falls away directly parallelling T_c, whilst the pseudogap grows monotonically. The results for the superconducting gap accord with existing data from specific heat [3], penetration depth [4], Andreev reflection [5], Raman spectroscopy [6], tunnelling [7] and other probes sensitive to the condensed state. What the new ARPES experiments provide is a more extended view of what was to be gathered from earlier ARPES [8, 9] and energy-resolved STM work [10], in particular of the strongly anisotropic distinctions current in the physics operative within the nodal and antinodal sectors. It has for some time been apparent that the action nearer the nodes is not especially unusual (except in degree) and that the remarkable input to the HTSC phenomenon comes with the special activity registered in the antinodal, saddle point regions. Nearer the nodes there exists rather classical fermionic behaviour, with a d-wave gapped Fermi surface, under impress of the superconductivity [11]. In the antinodal regions, however, there is active a chronic scattering which even in the normal state acts to precipitate disintegration there of the Fermi surface [12, 13]. This developing incoherence attaches a positive Seebeck coefficient to all under- and optimally-doped HTSC systems below 300 K [14]. The Seebeck coefficient along with the Hall coefficient both show highly anomalous temperature dependencies [15–17], as does the very non-standard, highly anisotropic resistive scattering [18–21]. This abnormal behaviour centred upon the saddles has been discussed by the author in a whole series of papers since 1987 [22–33]. These expound cuprate HTSC phenomena in terms of inhomogeneous, negative-U, fermion-to-boson interchange, seen as arising within a system driven to BCS/BEC crossover by 'accidentally' presenting a narrow (Feshbach) resonance between E_F and the local negative-U state in question (see final figure in [26]). The latter is presented as the double-loading fluctuation in electron content

 © 2008 IOP Publishing Ltd Printed in the UK

of a Cu_{III} coordination unit from p^5d^9 to p^6d^{10} (or in the notation of [23] $^8Cu^0_{III}$ to $^{10}Cu^{2-}_{III}$). In the most recent of the above papers [33], while the promoted superconducting condition around the nodes is as usual regarded as covered by B_{1g} symmetry, the local pair action instigating this low temperature state and centred upon the saddle hot spots takes geometrically related A_{1g} symmetry, very suited to coordination unit breathing and closed-shell configuration physics. The bosonic local pair states established from the saddle region quasiparticles can be held either within the overall superconducting condensate or be external to it/excited from it. The two conditions for local pairs are seen as engendering the two distinct types of bosonic mode sensed experimentally (see [31]). The first is in evidence in the mode-coupled physics evident in low temperature Raman [34, 35], EELS [36], ARPES [37] and inelastic neutron scattering work [38, 39], whilst the second, more k-dependant mode is met with in gigahertz spectroscopy [40] and energy-resolved scanning tunnelling microscopy [41, 42]. The presence of local pairs to well above T_c is signalled too by the Nernst coefficient results [43, 44]. The general positioning of the negative-U state as near to resonance with E_F is, I have claimed in [28], extensively supported by the results of laser pump–probe work [45, 46] and other specialist optical data [47–49]. The extracted net value of Hubbard U_{eff} for the Cu_{III}-site is ≈ -3.0 eV per pair, or -1.5 eV per electron [28].

When underdoped, the negative-U local pair state ends up being stationed some tens of meV below E_F, at binding energy $\mathcal{U}(p)$. With increased doping level, p, the local pair state rises slowly with respect to E_F (i.e. $\mathcal{U}(p)$ will diminish) as the general level of metallicity increases. The *local* Madelung potential around those copper centres transiently driven towards formal trivalence (through the oxidative mixed-valent 'doping' in the 'double' Mott system) becomes steadily screened away, permitting the material to relax towards a more customary, homogeneous, Fermi liquid behaviour. However in $(La_{2-x}Sr_x)CuO_2$ (LSCO) that condition still is not fully attained even by $p = 0.3$, beyond where HTSC itself has been relinquished [50]. Indeed in this higher range local moment magnetism starts to re-appear [51, 52].

'Optimal doping' enfolds several factors. Firstly, because it is found in all HTSC systems at virtually the same doping level ($p = 0.155$), this must reflect basic key geometrical constraints; namely (i) for the random case, the first appearance of 2D percolation paths over Cu–O coordination units immediately proximate to the charge centres within the random dopant array (see figure 4 in [23]), and (ii) for the fully stripe-organized case, the stripe crossing-point cluster-centring condition of figure 4 in [32]—see section 3 below. Secondly one is confronted by the marked effect brought by changes in counter-ion selection upon the T_c^{max} attainable within a particular system. What alteration in the counter ions (Ca, Sr, Ba, La, Hg, Tl, Pb, Bi, etc) involves is modification to the level of ionicity and screening within the crucial CuO_2 layers. This proceeds as follows. The ionicity of the counter-ion sets the degree of covalent mixing of that ion's s- and p-states with the oxygen sublattice s- and particularly p-states, the principal contributors to the main valence band. The latter, predominantly oxygen-based states, then hybridize with the copper d- and s-states by an amount fixed by the 'interim' energy separation. This hybridization then determines the ultimate relative positions and widths of the states of immediate relevance to HTSC. Foremost are the $d_{x^2-y^2}$ symmetry, $pd\sigma^*$ (antibonding), basal-plane conduction-band states. The $d_{x^2-y^2}$ band in the present structures becomes totally elevated above the d_{z^2} symmetry, apical, antibonding σ^*-band through Jahn–Teller distortion. This local distortion reflects complete filling of the d_{z^2} state with (sub)half-filling of its $d_{x^2-y^2}$ partner state in the $pd\sigma^*$ set of antibonding bands. The strong apical elongation of a CuO coordination unit indicates not only that the d_{z^2} state will locally be significantly less antibondingly elevated than the basal $d_{x^2-y^2}$ state, but also means that the lattice has become basally compressed, since the Jahn–Teller distortion is volume conserving. Such compression brings greater dispersion to the basal $d_{x^2-y^2}$ band than would result in a less 2D situation. The increased dispersion brings in turn enhanced tendency to resonant valence bond (RVB) formation within the conduction band and the constraint of free magnetic moments. Free moments form of course the principal agent for pair breaking in superconducting systems. One can appreciate then the delicate control which selection of the counter ions has over T_c. It dictates the absolute value of the chemical potential/work function and, via the level of screening at a given p value, the degree of metallicity and magnetic moment suppression. Presently $HgBa_2Ca_2Cu_3O_{16+\delta}$ with a certain amount of fluorine substitution offers the most advantageous combination towards elevating T_c^{max} [53]. However room still exists for ingenuity here as the various parameters are so sensitive and strongly intertwined. The increased basal compression brought by additional fourfold coordinated CuO_2 layers plus Ca (say in HBCCO-1212 versus HBCO-1201) succeeds in raising T_c^{max} only for as long as such insertion does not lead to dispersal of the effect of the dopants away from the critical outer layers of the complete CuO sandwich [54, 55]. T_c^{max} for Bi-2201 falls far below that for Bi-2212 because bismuth imports particularly advanced covalent admixing. At the opposite ionic extreme with $(Na_{2-x}Ca_x)CuO_2Cl_2$, the metallicity becomes so diminished that the Fermi surface begins seriously to disintegrate there once below $x \sim 0.12$ [56], and magnetic [57] and checkerboard states [32, 58] arise to counter HTSC.

2. Regarding the recent ARPES results of Tanaka *et al* and Valla *et al*

We may now turn to examine the results and discussion appearing in the recent ARPES papers from Tanaka *et al* [1] and Valla *et al* [2] plus the accompanying Comment by Millis [59]. From the position outlined above it is to be expected, and indeed found, that the situation upon moving into the underdoped region is characterized by two divergent energy scales, $\Delta(p)$ and $\mathcal{U}(p)$. Under falling p the instigating negative-U state's *binding* energy, $\mathcal{U}$, (below E_F) of the antinodally created local pairs will grow, whilst $\Delta(\phi)$, the fermionic gapping induced around the nodal directions, will

diminish, as coupling between the negative-U states and the fermionic open band drops away. Conversely towards optimal doping, $\mathcal{U}$ and Δ (or rather Δ as extrapolated to the d-wave maximal value of $\Delta(\phi \to 0)$ within the saddles) draw together, as $\mathcal{U}(p)$ becomes steadily lessened under metallic screening, and the strikingly small coherence lengths expand somewhat.

The peaks decorating the ARPES response customarily are presented as classical coherence peaks, but such a view has been contested by the present author in [33]. There it is proposed that for these very highly correlated systems the ARPES emission process becomes coupled to the c-axis charge plasmon, strongly in evidence in FIR [60] and Raman [35] work. Notice how in [1] the so-called 'coherence peak' stays at finite energy in the ARPES spectrum right round to the nodal point itself, and furthermore grows sharply in size and definition with rising p as T_c is advanced from 30 to 40 to 50 K over the UD series of $Bi_2Sr_2(Ca/Y)Cu_2O_8$ samples used. Once away from the nodal region and into the saddle region of advanced incoherence it is observed that this peak becomes much broadened. The peak's binding energy moreover becomes so large (>30 meV) that it cannot be associated directly with $\Delta(\phi)$. If it were taken simply as $\Delta(\phi)$ the extrapolated saddle peak energies would correspond to $2\Delta^{\max}(p)/kT_c(p)$ standing much in excess of what techniques more directly sensitive to the superconductivity itself support, namely $2\Delta^{\max}/kT_c \sim 5\frac{1}{2}$. Hence by the 'antinodal' direction the ARPES peak has lost all relation to Δ, the gap feature of a classical, non-local pair (BCS) superconductor. It has come to lack due pair-coherent aspect, and is in this mirroring the incoherence evident there too in the single particle spectrum. Both are expressions of the local pair creation and annihilation scattering out of and back into these zone boundary, saddle point states. As then is to be anticipated the broad peak feature in the ARPES spectra at the saddles shows little or no temperature dependence across T_c, unlike with the peaking found once away from these key regions.

3. 2-q striping and localization

The above incoherence, as noted earlier, is much more developed towards the more ionic limit of the HTSC systems, and in $(La_{2-x}Ba_x)CuO_4$ one encounters the well-known complete loss of superconductivity close to $x = p = \frac{1}{8}$. The latter event doubtless is encouraged by the structural complications shown by this particular system, with its HTT to LTO (at T_{d1}) to LTT (at T_{d2}) set of low temperature, coordination-unit-tilted, superstructures [61]. These typify the ferroelectric/ferroelastic-type ground-state adjustments of ionic oxide systems, especially those supporting Jahn–Teller distortion and orbital ordering. This is what brought Bednorz and Müller to examine these materials in the first place, with an eye towards soft-mode-driven superconductivity. Being mixed-valent, there exists in the HTSC cuprates the added propensity to support charge ordering, present again in isostructural but Mott-insulating $(La_{2-x}Ba_x)NiO_4$. It is well-known that in LBCO, etc a residue of such 'stripe phase' behaviour persists, dynamically at least, notably in inelastic neutron and x-ray scattering results. What is found at $x = \frac{1}{8}$ in LBCO (although not quite in LSCO) is that this charge ordering becomes static. The charge order brings in its wake magnetic ordering of appropriate $8a_o$ periodicity, as the two valence sites segregate to leave areas of Cu(II) more strongly and systematically coupled. All this is well supported by magnetic susceptibility [62], μSR [63], NMR/NQR [64], 2-magnon Raman work [65], etc, etc. The elimination at $p = \frac{1}{8}$ of RVB coupling, with the removal of the low energy spin gaps that elsewhere characterize the HTSC cuprates, is much furthered by perturbing the CuO_2 layers via Zn substitution [66] or the application of a magnetic field [67].

Back in 1988 in [24] I queried whether what was happening in LBCO near $p = \frac{1}{8}$ might not actually be Wigner crystallization of the quasiparticles to create a 45°-rotated, $(2\sqrt{2} \times 2\sqrt{2}a_o)$ charge order in empathy with the LTT lattice superstructure formed below 60 K. However as the pseudogapping (at least in its lower energy range) has become taken as associated with the superconductive pairing, one questions whether the incoherence developing in the Fermi liquid might not actually reflect a crystallizing out of pairs rather than just quasiparticles [68]. In figures 1(b) and (c) the above two events are depicted against a background of charge striping such as would hold were the system at $p = \frac{1}{8}$ to behave as when away from this special, lattice commensurate, doping level. At the $x = \frac{1}{8}$ stoichiometry the measured $8a_o$ periodicity dictates that sites internal to the domain wall stripes alternately carry Cu(II) and Cu(III) charge loadings, as in figure 1(a). The stripe background to this figure will immediately be seen as 2-**q** in form rather than of the customary uniaxial 1-**q** dispensation. This follows my understanding of these events presented initially in [26, 27] and subsequently much developed in [32]. In figure 1(a) one may immediately pick out for these mixed-valent 'metals' the pertinent, nodally oriented, 'rivers of charge'.

I am aware, after Fine's work along similar lines, pursuing somewhat different arguments [69], that the matter of 2-**q** domaining has recently been re-addressed, in particular by Christensen *et al* [70]. From the latters' spin-polarized neutron diffraction data it is evident that 2-**q** domaining is indeed a viable option, although not one with basally collinear spin patterning such as that portrayed by Fine in [69]. In my figures of [32] I chose not there to address the matter of the anisotropic constraints operative upon the spin axes in the divalent domains. The spins were drawn as if assuming the c-axis direction, although in La_2CuO_4 itself they align almost in the basal plane [71]. For the mixed-valent striped case, as indicated in figure 8 of [26], the probable outcome, under the magneto-elastic forces set up by the domain walls, is for the basically antiferromagnetic spin arrays either to be distorted hedgehog-like towards the walls or be driven into circulations of spin directed as far as possible parallel to the walls. The existence of very strong magneto-elastic forces in LBCO in the vicinity of $p = \frac{1}{8}$ is well established from ultrasound data [72], and was discussed in sections 4 and 5 of [26]. Such spin conformations now are portrayed in figure 2 below for the revised 45° orientation of 2-**q** domain walling developed in [32]. It is my belief these spin structures match the refined neutron diffraction data newly obtained by Christensen *et al* [70]—see later in section 5.

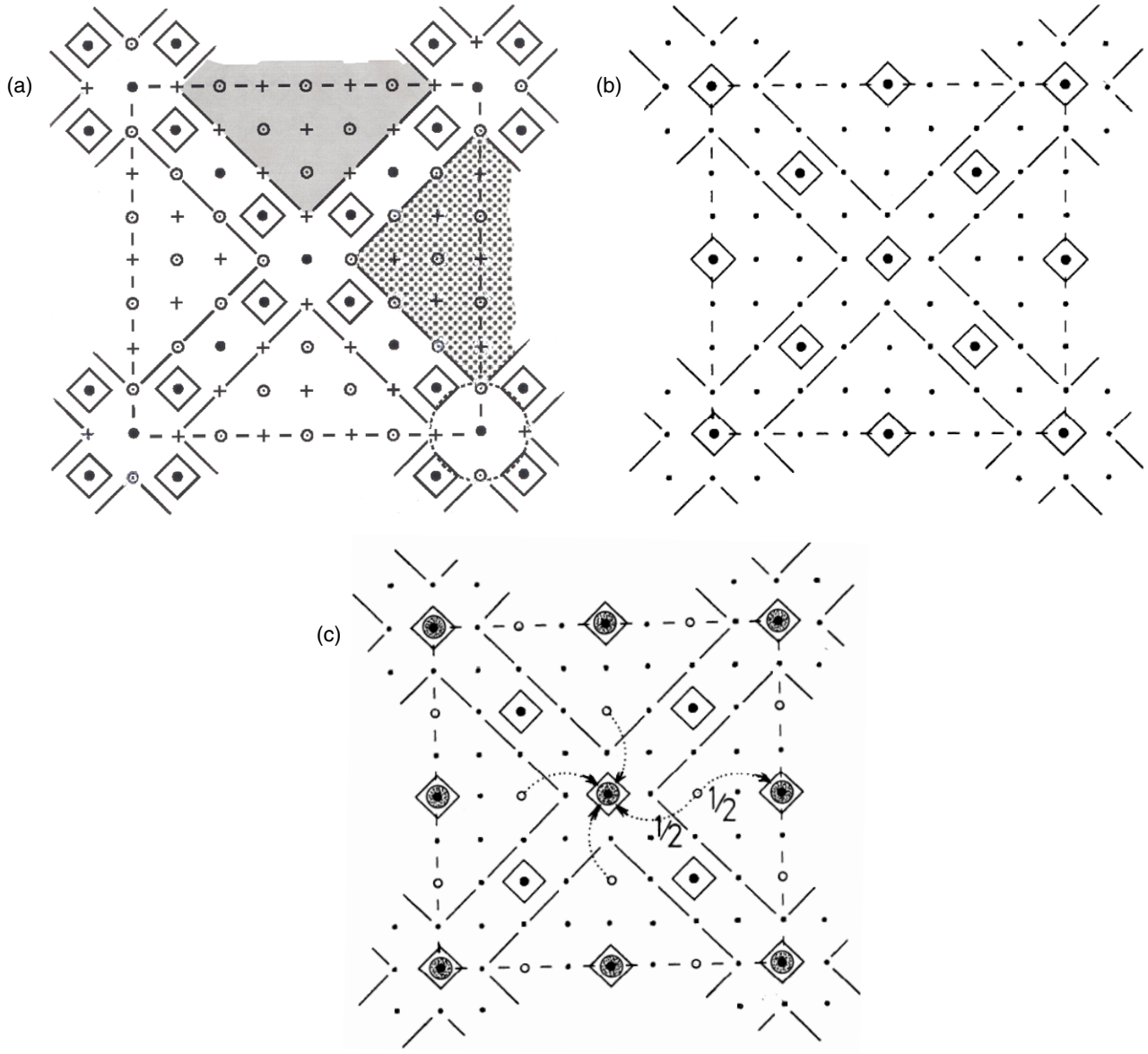

Figure 1. (a) The 2-**q** diagonal stripe array for $p = \frac{1}{8}$, as introduced in [32]. The $8a_o$ supercell detected for LBCO by elastic x-ray and neutron diffraction sets the scale to this figure, in which the copper atom sites predominantly feature. Cu(II) sites in the domains between the stripes are marked + and ⊙ to indicate their antiferromagnetically coupled status, whilst in the stripes non-magnetic Cu(II) sites ● alternate with Cu(III) 'hole' sites ◇. The latter sites are framed by small squares marking their four basal coordinating oxygen locations. The stripe crossing points are each decorated by four holes to yield an overall supercell that is face-centred. The inner domains are alternately dominated by 'up' and by 'down' spin electrons, as indicated by the areal shading, once again defining a face-centred array (but 45°-rotated). The $\sqrt{5}a_o$ circle at the bottom right marks the centre of negative-U activity at the stripe crossing-points with their enhanced Madelung potential. The stripes provide the diagonal (nodal) coherent 'rivers of charge', whilst the domains supply heavy/incoherent x- and y-axis saddle electrons to the negative-U centres for pairing. This patterning becomes completely frozen in $x = \frac{1}{8}$ LBCO below the LTT tilt transition at T_{d2}, resulting in the loss of HTSC behaviour. (b) Postulated Wigner crystallization of quasiparticle holes at $p = \frac{1}{8}$, as set against background of the diagonal 2**q**-striping of figure 1(a). To reach this pattern from figure 1(a) requires that the Cu(II)/Cu(III) phasing between stripes be slipped by π so that a hole sits at the stripe crossing points. The 'surplus' hole per $8a_0$ cell then is accommodated at the supercell centre to reach the regularized hole array presented. (c) Postulated Wigner crystallization of *electron* pairs at $x = \frac{1}{8}$, again employing 2**q**-diagonal striping as reference background. This condition would require the net transfer of two electrons into those Cu(III) sites in figure 1(b) formerly occupying the symmetric sites at the domain corners and centres as is indicated. Besides being symmetry-wise rather odd, this transfer effectively amounts to a disproportionation process for which there is no evidence elsewhere in copper chemistry (unlike silver and gold).

Let us return to the matter of Wigner crystallization, whether of quasiparticles or of pairs, viewed now against this setting of rotated 2-**q** domaining. To reach uniform Wigner crystallization of the holes starting from figure 1(a) calls simply for the relative phasing of charge alternation at the crossing points of the diagonal stripes to be slipped by π, with the 'surplus' hole generated then accommodated at a domain centre (figure 1(b)). It is perhaps more in line however with present work that what might crystallize are not the quasiparticles themselves, i.e. the holes, or even hole pairs, but,

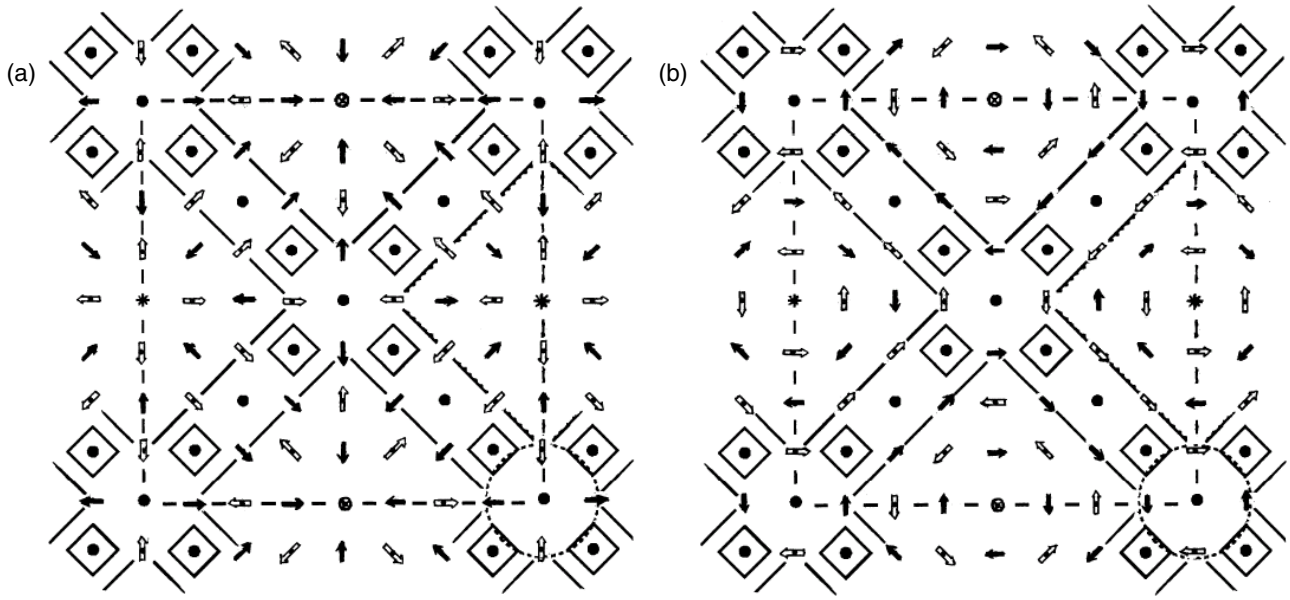

Figure 2. (a) Spin array of figure 1(a) as constrained by Jahn–Teller supported magneto-and ferroelastic forces established at boundaries of mixed-valent diagonal striping. The small arrows show the directed horizontal components of the spins at the domain sites. In this hedgehog array of spins the latter are constrained as far as possible to set orthogonal to the stripes. Alternate domains, following the experimentally endorsed spin discommensuration sequencing of figure 1(a), are dominated by outwardly and then inwardly directed basal spins. Polarized neutron experiments on YBCO [82] suggest that the spins actually are aligned closer to the vertical than to the horizontal. The saddle mirror remains intact with this spin array, but the original diagonal lattice mirror is broken by this pattern. (b) Partner figure to (a) with the spins now constrained as far as possible to set with their basal components parallel to the charge striping. These circulations of spin alignment this time conserve the diagonal mirrors but break the axial mirror operations. It is this circumstance which, unlike that of figure (a), matches the magnetic circular dichroism data obtained by Kaminski *et al* [79].

as pointed to above, *electron* pairs. These pairs, materializing at the Cu(III) negative-U centres, potentially could lock onto the stripe crossing-points and set up the 4×4 electron pair array shown in figure 1(c). This in fact would constitute not so much a directly correlation-driven crystallization of pairs as one initiated by ferroelastic forces, paralleling the magneto-elastic forces that organize the spin arrays. As with the stripes themselves (and indeed with the very elevation of the $d_{x^2-y^2}\sigma^*$-band to stand alone) the above forces emanate largely from the strong Jahn–Teller-based distinction between Cu–O coordination unit geometries under d^8, d^9 and d^{10} site loadings. The tilts of the $^9Cu_{II}$ units in the LTO and LTT low temperature structures accommodate there the strong apical (c-axis) elongation. This structural extension, whilst injecting such complexity into LBCO at $x = \frac{1}{8}$, becomes in $HgBa_2CuO_{4+\delta}$ of great benefit in contracting a_o and thereby promoting RVB over ungapped, antiferromagnetic, spin coupling. In $p = \frac{1}{8}$ LBCO, in contrast, the greater ionicity leads to a resurgence of antiferromagnetism, which contributes much to preventing superconductivity being promoted over the Fermi sea.

The negative-U scenario developed in [22–33] is, recall, one of electron pairs not hole pairs, the former associated with the attainment within a local negative-U state coordination unit of the fully closed-shell p^6d^{10} condition, the $^{10}Cu_{III}{}^{2-}$ state. The proximity to this closed-shell condition is what makes the cuprates unique (except for the rather similarly placed mixed-valent bismuthate family $(Ba/K)BiO_3$, etc). It is this closed-shell circumstance which relates these systems to the phenomenon of charge disproportionation. However, as stated from the outset, lattice-constrained electron pairing emerging under static charge disproportionation is the last thing one wishes in fact to encounter when hunting down HTSC. Static charge disproportionation becomes in AgO representable, within the notation of [22], by

$$^9Ag^0_{II} + {}^9Ag^0_{II} \rightarrow {}^{10}Ag^0_{I} + {}^8Ag^0_{III}.$$

The transfer here over to the strongly semiconductive end-point is considerably advanced by virtue of the lattice structure acquired. In AgO, alongside the large monovalent coordination unit, one has for the Ag(III) the often seen square-planar d^8 unit of semiconductive d^8 Pd(II)O, etc. What a mixed-valent composition accomplishes with the HTSC cuprates and the bismuthates, due to their intrinsic structural disorder, is a forestalling of any such drive to adopt a statically disproportionated lattice structure. As the amount of mixed-valent doping with its attendant metallicity is reduced any latent tendency towards charge disproportionation will become less frustrated. What appears in figure 1(c) for $p = \frac{1}{8}$ LBCO may in fact be viewed as a frozen disproportionation wave rather than an electrostatically-driven quasiparticle pair crystallization. By concentrating upon a 4×4 electron-pairing square repeat of 16 unit cells, it is noted that the process indicated amounts to adjusting from $(2d^8 + 14d^9)$ to $(3d^8 + 12d^9 + 1d^{10})$; i.e. a net shift from $2d^9$ to $(d^8 + d^{10})$—as under disproportionation.

Both above pictures, figures 1(b) and (c), indeed then hold undesirable characteristics. While a loss of superconductivity

may well follow from such charge 'crystallization', it would come at the cost of disassociating the $\frac{1}{8}$ material from its flanking compositions. In particular it would override the continuity evident in the IC neutron *spin* diffraction results, below as above $T_{d1,2}$. There is too the implication that the outcome would be far less metallic than actually proves the case. It is felt the above notions of Wigner crystallization have emerged from over-emphasis upon the holes and upon the stripe array. If we refocus on the interior of the domains, and on the electrons based there, we will come to a much more satisfactory perspective on events.

4. Consequences for the optical, magnetic, transport and tunnelling results

What the resurgence of magnetic behaviour at the congregating d^9 sites near $x = \frac{1}{8}$ signals is a move towards localization for the electrons and specifically those of the domain. While $\rho(T)$, $R_H(T)$ and $S(T)$ do not indicate the onset of full-blown Mott localization, it is very evident that a form of weak localization is being encountered. While $\rho(T)$ shows just a small upward step discontinuity of <5% as T passes below T_{d2} [73], by contrast $R_H(T)$ falls more sharply down through zero than is found away from $p = \frac{1}{8}$ [74], and $S(T)$ [75] also advances its departure from mounting positive values. What is implied is that the inner domain is losing coherent electronic contact with the stripes, as the lattice strain at the domain boundaries grows under the developing charge segregation. The Cu(II) patch is coming to define a self-trapped, meso-scale, charge defect, with a binding energy of the order of a few kT. (Note $T_d \approx 60$ K is $\equiv 5$ meV). One might ask here if there is any evidence for such self-trapping showing up in the far-infrared (FIR) optical spectrum—and the answer is yes. The single crystal reflectivity work on $x = \frac{1}{8}$ LBCO (versus LSCO) published recently by Homes *et al* [76] lends full support to such an interpretation. To fit their FIR data necessitates that the optical conductivity be apportioned between a coherent, Drude-like component, such as would encompass the near-nodal charge, and a significant incoherent, constant component, as would deal with the saddle electron **k** states. A Kramers–Kronig analysis made in the above form reveals a very significant spectral weight loss at energies below 200 cm^{-1} ($\equiv$ 25 meV or 300 K), this setting in sharply at T_{d2}. n_D, the coherent charge density, becomes by 4 K reduced to just 25% of its value at 60 K. At the same time, as is very evident from the rapidly sharpening, very low frequency Drude tail to the optical conductivity, the optical scattering rate derived for the more coherent states accelerates its general fall once $T < T_{d2}$. At T_{d2} note $1/\tau_D$ (equal there to 108 cm^{-1}) is equivalent to $2\frac{1}{2}kT_d$. Such a scattering rate translates into a characteristic time of 2×10^{-12} s, this speaking of a process that is phonon limited. As the rate-determining charge exchange between the domains and stripes starts to freeze out strongly below T_{d2}, this change becomes apparent in the accelerated *reduction* in scattering rate for the residue of coherent electrons. The latter stripe-based carriers now are less perturbed by ingress of heavy electrons from the domains. As the supply of the latter electrons to the negative-U centres dries up, so too will, of course, the rate of generation of local pairs, and with this ends the capacity to project superconductivity back into the domains. The HTSC cycle collapses.

What are the observed consequences of the above for the non-superconducting $x = \frac{1}{8}$ material? It has become clear that the events in LBCO are not simply the outcome of the adoption of LTT superlattice structuring alone. Indeed the effects extend through to temperatures appreciably above T_{d2}. Correspondingly in LSCO, while the application of a magnetic field is known to have virtually no effect upon the lattice softening associated with the incipient low temperature superlatticing [72], it has been found to have a big effect upon the magnetic and superconductive action around $x = \frac{1}{8}$ [67]. The LTO and LTT crystal structure transformations per se clearly are not greatly affecting the band structure at E_F, as evidenced also by the $\rho(T)$, $S(T)$ and $R_H(T)$ plots showing only rather subtle changes at T_d. The $x = \frac{1}{8}$ transport data indeed step surprisingly little out of line in general magnitude with what is found for the flanking compositions where superconductivity arises. What do alter are the EXAFS-recorded Cu–O bond lengths, as might be anticipated for a charge localization process quasistatic in nature [77]. The main effect of the low temperature changes around $x = \frac{1}{8}$, one perceives, is to introduce a somewhat augmented localization, and with this an increase of singlet pair breaking for the Fermi sea based condensate. It is not that the negative-U pair states have disappeared or have been markedly shifted in energy away from resonance and thereby becomes ineffective at inducing superconductivity. Rather the $\frac{1}{8}$ condition chiefly entails a slower inter-subsystem charge fluctuation rate and a faster depairing rate.

Whilst the B_{1g} d-wave superconductive gap is depressed, this does not mean the A_{1g} gapping associated with the negative-U state will likewise have lessened. Long ago it was shown by Maggio-Aprile and co-workers [78], employing STM to examine the situation inside magnetic field vortices in HTSC materials, that, with the re-institution there of magnetic behaviour, the quenched superconductivity and associated loss of gapping were not accompanied within the vortices by any simultaneous elimination of the larger energy 'pseudogap' peak. The latter negative-U feature was found to remain in evidence at the same energy there as in the field-free condition. It is this same 'pseudogap' feature which now is reported on by Valla *et al* [2] in the new ARPES work for $x = \frac{1}{8}$ LBCO. The observed peak energy of 20 meV stands entirely in agreement with the 'pseudogap' energy in the antinodal ARPES spectrum of underdoped LSCO reported by Tanaka *et al* in [1], and present there to well above T_c. It is a feature that in the underdoped material stands well above the 2Δ values relating specifically to the onset of superconductivity itself. It appears to the author there is no problem whatsoever in embracing all these findings within the scope of the present, inhomogeneous, negative-U scenario.

5. Encompassing the magnetic circular dichroism and related results

A final outcome to emerge from the above considerations is an explanation for the magnetic circular dichroism (MCD) found

in underdoped HTSC cuprates [79]. The motivation for the MCD experiment came from Varma [80] upon contemplating whether the pseudogap state might not involve a subtle symmetry breaking, with associated order parameter, upon engagement at T^*, rather than simply to be a fluctuational condition. Because the lattice structure/symmetry had long been deemed unchanging at T^*, the natural symmetry breakage postulated was of time reversal symmetry: TRSB customarily is associated with spin. Since T^* would seem from neutron diffraction not to involve a standard magnetic transition, it was proposed that, if experiment were to pick up a weak symmetry breakage, it might actually be indicative of spontaneous current-loops occurring at the unit cell level. The latter, of course, would be associated with weak local magnetic moments, and possibly also with zero net magnetization, accounting thereby for the absence of any betrayal hitherto of their presence. The fact that in [79] Kaminski *et al* do from their circularly polarized ARPES experiment on underdoped BSCCO appear to have recorded a small but well-structured MCD response (below T^*, as T_c), absent with overdoped BSCCO, has lent some support for there being an exotic current-loop precursor condition to UD HTSC. However, it is my belief now that interpretation of this finding is a good deal more prosaic, and that it is associated with the spin structures emerging in conjunction with the diagonal 2-**q** charge striping met with above. Moreover the MCD results will permit us to make selection between the two magneto-elastically constrained possibilities presented in figure 2 above in favour of figure 2(b)—the circulatory spin pattern.

One additional result necessary to incorporate prior to considering the details of this MCD work is that evidence for relatively weak magnetic ordering activity now has been secured below T^* in underdoped YBCO also. The spin diffraction recently registered there by Fauqué *et al* [81] via elastic spin-polarized neutron scattering is quasistatic on the neutron diffraction timescale of 10^{-12} s. Thus T^* would appear to be where stripe ordering starts to become organized. The 'ordered' moments reported up in this region are only around 0.1 μ_B but manifest quite appreciable magnetic coherence lengths of 50 Å plus (i.e. three to four diagonal stripe domains). As noted already, the application of a magnetic field enhances site moments, and hence it is not surprising Shi *et al* [82] from their measurement in a field of 8 T of the infra-red Hall effect make now additional report of Faraday rotation and circular dichroism in underdoped LSCO right through to 300 K. The new neutron work by Fauqué *et al* [81] would suggest that with YBCO the freezing magnetic moments tilt very substantially out of the basal plane, and probably lie closer to the c-axis than to the a, b plane. YBCO with its chains of course is not the archetypal HTSC material, but one may contemplate the spins strongly tilted out of the basal plane too in the other HTSC systems under the strong magneto-elastic action of the stripes. Hence figures 2(a) and (b) represent only the orientation of the horizontal components to the site spins. These arrays on cooling settle steadily towards a 'spin-gapped' ground state as RVB develops.

We now may examine in detail what Kaminski *et al* find in the MCD ARPES experiment [79]. Their set up is so configured that across a standard c-axis structural mirror plane the relative intensities of right-and left-circularly polarized (RCP/LCP) ARPES signals swap over at **k**-vectors lying precisely on the mirror plane. *Over*doped samples always yield just such a 'null' result, both for the axial and the diagonal mirror planes of the (pseudo-tetragonal) crystal structure. However the various *under*doped samples examined all produce, once below T^*, an MCD signal indicative of TRSB. This symmetry breakage is deduced from experiment to relate uniquely to the axial (saddle direction) mirror of the basic structure and not to the diagonal mirror. The distinguishing MCD response involves a small transverse offset (2.3°) for the RCP/LCP equal intensity crossover **k**-point away from the relevant vertical mirror plane. Right at the mirror there occurs an intensity difference between the RCP and LCP ARPES signals. Rotating the sample by $\frac{\pi}{2}$ sees the sign of this intensity difference reversed. The observations establish that the magnetic constraints on the signal are such that TRS breakage of the basic symmetry arises in regard to the axial mirror of the crystal structure but not to the diagonal mirror. Inspection of figures 2(a) and (b) then makes apparent it is the latter of these two circumstances, the circulatory arrangement, which must hold. In retrospect this is not an unreasonable outcome. We find with choice 2(b) that the spins indeed reflect across the diagonal plane but not across the axial Cu–O-bond/saddle mirror, just as the ARPES experiment implies. (With 2(a) the converse holds.) Note that the spin arrangement in 2(b) (as in 2(a)) exhibits antiphase (spin discommensurate) character along the *axial* directions across the stripe crossing points, as supported by early neutron diffraction work. Across individual diagonal stripes there occurs a mirror relationship in figure 2(b) that is absent in figure 2(a). The repeat pattern of *spin* domains is in each case face-centred and bears a $\sqrt{2}$ relationship to the *hole charge* patterning. The latter is itself face-centred, but now with regard to the overall $8a_o$ axial supercell. It is this face centring which is responsible for the systematic absences in both spin and charge diffraction spotting pointed to in [32].

6. The way forward and summary

It is fascinating to see again how the twelve inherent aspects to HTSC cuprate physics identified in 1987 in [22, 23] come through in practice to build a situation of such rich complexity. From this platform it surely is time now to probe once more the actual dynamics of the superconducting process—the heart of the matter—via the employment of pump–probe laser techniques. The earlier such experiments of [46] and [48] (and what was made of these in [28]) has been added to recently by the results of [83]. This work should now be made to embrace what is known regarding the stripe condition in optimally and underdoped material. The key aim remains to clarify the source of the observed, three-component, dynamical behaviour, and to ascertain whether its relationship to the inhomogeneous two-subsystem/domain structuring of these materials will indeed continue to sustain the conclusions drawn in [28], upon which so much in the current paper and its predecessors rests. It is hoped finally that somebody will take up the challenge

made in [33] to examine theoretically the present negative-U exposition using cluster dynamical mean field techniques.

In summary we have seen how the present negative-U/BCS-BEC crossover modelling of HTSC cuprate phenomena provides ready explanation for the observed dual energy scales apparent in underdoped ARPES results. With underdoping the negative-U state binding energy $\mathcal{U}$ grows, as tracked by T^*, whilst the induced superconductive gapping Δ of the nodal states falls away as T_c. This divergent behaviour continues through to localization. Partial localization near $p = \frac{1}{8}$ is encouraged by the application of a magnetic field and by the strain fields associated with valence segregation into striped arrays, very pronounced in LBCO. The effects of such localization of the saddle quasiparticles is very apparent in far-IR spectroscopy. The heavy scattering experienced by these latter states marks the seat of local pairing in k-space. In direct space the 2**q** stripe modelling developed would see local pairing as being most favourably secured at the stripe crossing points. The magnetic organization of the inner parts of the stripe domains in underdoped material is shown to support the right symmetry characteristics to be responsible for the observed magnetic circular dichroism.

Acknowledgments

The author gratefully acknowledges receipt of a University Fellowship, permitting this work to be carried forward. My thanks again go to the members of the low temperature group in Bristol for their shared enthusiasm over all matters relating to HTSC.

References

[1] Tanaka K *et al* 2006 *Science* **314** 1910
[2] Valla T, Federov A V, Lee J, Davis J C and Gu G D 2006 *Science* **314** 1914
[3] Loram J W, Mirza K A and Cooper J R 1998 *Research Review 1998 HTSC* ed W Y Liang (Cambridge: IRC, Univ. of Cambridge) pp 77–97
Loram J W, Luo J, Cooper J R, Liang W Y and Tallon J L 2001 *J. Phys. Chem. Solids* **62** 59
[4] Panagopoulos C, Cooper J R and Xiang T 1998 *Phys. Rev.* B **57** 13422
[5] Deutscher G 1999 *Nature* **397** 410
[6] Devereaux T P F and Hackl R 2007 *Rev. Mod. Phys.* **79** 175
[7] Dagan Y, Krupke R and Deutscher G 2000 *Phys. Rev.* B **62** 146
[8] Shen K M *et al* 2005 *Science* **307** 901
[9] Kim T K, Kordyuk A A, Borisenko S V, Koitzsch A, Knupfer M, Berger H and Fink J 2003 *Phys. Rev. Lett.* **91** 167002
[10] Zasadzinski J F, Ozyuzer L, Coffey L, Gray K E, Hinks D G and Kendziora C 2005 *Preprint* cond-mat/0510057
[11] Tsuei C C and Kirtley J R 2000 *Rev. Mod. Phys.* **72** 969
Tsuei C C, Kirtley J R, Hammerl G, Mannhart J, Raffy H and Li Z Z 2004 *Phys. Rev. Lett.* **93** 187004
[12] Yoshida T *et al* 2006 *Phys. Rev.* B **74** 224510
[13] Lee W S *et al* 2006 *Preprint* cond-mat/0606347
[14] Wilson J A and Farbod M 2000 *Supercond. Sci. Technol.* **13** 307
[15] Obertelli S D, Cooper J R and Tallon J L 1992 *Phys. Rev.* B **46** 14928
[16] Kubo Y and Manako T 1994 *Phys. Rev.* B **50** 6402
[17] Tsukuda I and Ono S 2006 *Preprint* cond-mat/0605720
[18] Hussey N E 2003 *Eur. Phys. J.* B **31** 495
Hussey N E, Takenaka K and Takagi H 2004 *Phil. Mag.* **84** 2847
[19] Hussey N E 2006 *J. Phys. Chem. Solids* **67** 227
[20] Abdel-Jawad M, Kennett M P, Balicas L, Carrington A, Mackenzie A P, McKenzie R H and Hussey N E 2006 *Nat. Phys.* **2** 821
Abdel-Jawad M, Analytis J G, Balicas L, Carrington A, Charmant J P H, French M M F and Hussey N E 2007 *Phys. Rev. Lett.* **99** 107002
[21] Hussey N E, Alexander J C and Cooper R A 2006 *Phys. Rev.* B **74** 214506
[22] Wilson J A 1987 *J. Phys. C: Solid State Phys.* **20** L911
[23] Wilson J A 1988 *J. Phys. C: Solid State Phys.* **21** 2067
[24] Wilson J A 1989 *Int. J. Mod. Phys.* B **3** 691
[25] Wilson J A 1994 *Physica* C **233** 332
[26] Wilson J A and Zahrir A 1997 *Rep. Prog. Phys.* **60** 941
[27] Wilson J A 1998 *J. Phys.: Condens. Matter* **10** 3387
[28] Wilson J A 2000 *J. Phys.: Condens. Matter* **12** 303
[29] Wilson J A 2000 *J. Phys.: Condens. Matter* **12** R517
[30] Wilson J A 2001 *J. Phys.: Condens. Matter* **13** R945
[31] Wilson J A 2004 *Phil. Mag.* **84** 2183
[32] Wilson J A 2006 *J. Phys.: Condens. Matter* **18** R69
[33] Wilson J A 2007 *J. Phys.: Condens. Matter* **19** 106224
[34] Puchkov A V, Timusk T, Karlow M A, Cooper S L, Han P D and Payne D A 1996 *Phys. Rev.* B **54** 6686
Puchkov A V, Basov D N and Timusk T 1996 *J. Phys.: Condens. Matter* **8** 10049
[35] Munzar D and Cardona M 2003 *Phys. Rev. Lett.* **90** 077001
[36] Li Y and Lieber C M 1993 *Mod. Phys. Lett.* B **7** 143
Li Y, Huang J L and Lieber C M 1992 *Phys. Rev. Lett.* **68** 3240
[37] Norman M R, Kaminski A, Mesot J and Campuzano J C 2001 *Phys. Rev.* B **63** 140508(R)
[38] Chung J-H *et al* 2003 *Phys. Rev.* B **67** 014517
[39] Pintschovius L, Reznik D, Reichardt W, Endoh Y, Hiraka H, Tranquada J M, Uchiyama H, Masui T and Tajima J 2004 *Phys. Rev.* B **69** 214506
[40] Corson J, Mallozo R, Orenstein J, Eckstein J N and Bozovic I 1999 *Nature* **398** 221
Corson J, Orenstein J, Oh S, O'Donnell J and Eckstein J N 2000 *Phys. Rev. Lett.* **85** 2569
[41] Hoffman J E, McElroy K, Lee D-H, Lang K M, Eisaki H, Uchida S and Davis J C 2002 *Science* **297** 1148
[42] McElroy K, Lee J, Slezak J A, Lee D-H, Eisaki H, Uchida S and Davis J C 2005 *Science* **309** 1048
[43] Wang Y, Ono S, Onose Y, Gu G, Ando Y, Tokura Y, Uchida S and Ong N P 2003 *Science* **299** 86
[44] Li L, Wang Y, Naughton M J, Komiya S, Ono S, Ando Y and Ong N P 2006 *Int. Conf. Mag. (Kyoto 2006)* (*Preprint* cond-mat/0611731)
[45] Stevens C J, Smith D, Chen C, Ryan J F, Pobodnik B, Mihailovic D, Wagner G A and Evetts J E 1997 *Phys. Rev. Lett.* **78** 2212
[46] Demsar J, Podobnik B, Kabanov V V, Wolf Th and Mihailovic D 1999 *Phys. Rev. Lett.* **82** 4918
Demsar J, Hudej R, Karpinski J, Kabanov V V and Mihailovic D 2001 *Phys. Rev.* B **63** 054519
[47] Holcomb M J, Perry C L, Collman J P and Little W A 1996 *Phys. Rev.* B **53** 6734
[48] Li E, Sharma R P, Ogale S B, Zhao Y G, Venkatesan T, Li J J, Cao W L and Lee C H 2002 *Phys. Rev.* B **65** 184519
Li E, Ogale S B, Sharma R P, Venkatesan, Li J J, Cao W L and Lee C H 2004 *Phys. Rev.* B **69** 134520
[49] Little W A, Holcomb M J, Ghiringhelli G, Braichovich L, Dallera C, Piazzalunga A, Tagliaferri A and Brookes N B 2006 *M2S-HTSC VIII (Dresden, July 2006)* (*Preprint* cond-mat/060853)

[50] Nakamae S, Behnia K, Mangkorntong N, Nohara M, Takagi H, Yates S J C and Hussey N E 2003 *Phys. Rev.* B **68** 100502(R)
[51] Nguyen N, Studer F and Raveau B 1983 *J. Phys. Chem. Solids* **44** 389
[52] Le Bras G, Konstantinovic Z, Colson D, Forget A, Carton J-P, Ayache C, Jean F, Collin G and Dumont Y 2002 *Phys. Rev.* B **66** 174517
[53] Monteverde M, Nunez-Regueiro M, Acha C, Lokshin K A, Pavlov D A, Putilin S N and Antipov E V 2004 *Physica* C **408–410** 23
[54] Kotegawa H *et al* 2004 *Physica* C **408–410** 761
[55] Majoros M, Panagopoulos C, Nishizaki T and Iwasaki H 2005 *Phys. Rev.* B **72** 024528
[56] Shen K M *et al* 2004 *Phys. Rev. Lett.* **93** 267002
[57] Ohishi K, Yamada I, Koda A, Higemoto W, Saha S R, Kadano H, Kojima K M, Azuma M and Takano M 2004 *Preprint* cond-mat/0412313
[58] Hanaguri T, Lupien C, Kohsaka Y, Lee D-H, Azuma M, Takano M, Takagi H and Davis J C 2004 *Nature* **430** 1001
[59] Millis A J 2006 *Science* **314** 1888
[60] Dordevic S V, Komiya S, Ando Y and Basov D N 2003 *Phys. Rev. Lett.* **91** 167401
Dordevic S V, Komiya S, Ando Y, Wang Y J and Basov D N 2003 *Europhys. Lett.* **61** 122
[61] Kimura H, Noda Y, Goka H, Fujita M, Yamada K, Mizumaki M, Ikeda N and Ohsumi H 2004 *Phys. Rev.* B **70** 134512
Fujita M, Goka H, Yamada K, Tranquada J M and Regnault L P 2004 *Phys. Rev.* B **70** 104517
Kimura H, Noda Y, Goka H, Fujita M, Yamada K and Shirane G 2005 *J. Phys. Soc. Japan* **74** 445
[62] Hücker M, Gu G D and Tranquada J M 2005 *Preprint* cond-mat/0503417
[63] Sonier J E *et al* 2006 *Preprint* cond-mat/0610051
[64] Singer P M, Hunt A W, Cederström A F and Imai T 2003 *Physica* C **388/389** 209
Singer P M, Imai T, Chou F C, Hirota K, Takaba M, Kakeshita T, Eisaki H and Uchida S 2005 *Phys. Rev.* B **72** 014537
Grafe H-J, Curro N J, Hücker M and Büchner B 2006 *Phys. Rev. Lett.* **96** 017002
Matsumura M, Inouchi K, Yamagata H and Sera M 2001 *Physica* C **357–360** 89
[65] Machtoub L H, Keimer B and Yamada K 2005 *Phys. Rev. Lett.* **94** 107009
[66] Adachi T, Omori K, Kawamata T, Kudo K, Sasaki T, Kobayashi N and Koike Y 2006 *Yamada Conf. LX, RHMF (2006) Preprint* cond-mat/0608440
Naqib S H, Cooper J R, Islam R S and Tallon J L 2005 *Phys. Rev.* B **71** 184510
[67] Chang J *et al* 2007 *Phys. Rev. Lett.* **98** 077004
Savici A T *et al* 2005 *Phys. Rev Lett.* **95** 157001
[68] Franz M 2004 *Science* **305** 1410
Chen H-D, Vafek O, Yazdani A and Zhang S-C 2004 *Phys. Rev. Lett.* **93** 187002
[69] Fine B V 2004 *Phys. Rev.* B **70** 224508
Fine B V 2007 *Phys. Rev.* B **75** 014205
[70] Christensen N B, Rønnow H M, Mesot J, Ewings R A, Momono N, Oda M, Ido M, Enderle M, McMorrow D F and Boothroyd A T 2006 *Preprint* cond-mat/0608204
[71] Thio T, Thurston T R, Preyer N W, Picone P J, Kastner M A, Janssen H P, Gabbe D R, Chen C Y, Birgeneau R J and Aharony A 1988 *Phys. Rev.* B **38** 905
Lavrov A N, Ando Y, Komiya S and Tsukada I 2001 *Phys. Rev. Lett.* **87** 017007
[72] Sakita S, Suzuki T, Nakamura F, Nohara M, Maeno Y and Fujita T 1996 *Physica* B **219/220** 216
See also Silva Neto M B 2006 *Phys. Rev.* B **74** 045109
[73] Adachi T, Kitajima N, Manabe T, Koike Y, Kudo K, Sasaki T and Kobayashi N 2005 *Phys. Rev.* B **71** 104516
[74] Noda T, Eisaki H and Uchida S 1999 *Science* **286** 265
Ono S, Komiya S and Ando Y 2007 *Phys. Rev.* B **75** 024515
[75] Sera M, Ando Y, Kondoh S, Fukuda K, Sato M, Watanabe I, Nakashima S and Kumagai K 1989 *Solid State Commun.* **69** 851
Yamada J, Sera M, Sato M, Takayama T, Takata M and Sakata M 1994 *J. Phys. Soc. Japan* **63** 2314
[76] Homes C C, Dordevic S V, Gu G D, Li Q, Valla T and Tranquada J M 2006 *Phys. Rev. Lett.* **96** 257002
See also Dumm M, Basov D N, Komiya S, Abe Y and Ando Y 2002 *Phys. Rev. Lett.* **88** 147003
[77] Saini N L, Oyanagi H, Wu Z and Bianconi A 2002 *Supercond. Sci. Technol.* **15** 439
Oyanagi H, Saini N L, Tsukada A and Naito M 2006 *J. Phys. Chem. Solids* **67** 2154
[78] Maggio-Aprile L, Renner C, Erb A, Walker E and Fischer Ø 1995 *Phys. Rev. Lett.* **75** 2754
Fischer Ø, Kugler M, Maggio-Aprile I, Berthod C and Renner C 2006 *Preprint* cond-mat/0610672
[79] Kaminski A *et al* 2002 *Nature* **416** 610
[80] Varma C M 2000 *Phys. Rev.* B **61** R3804
Simon M E and Varma C M 2002 *Phys. Rev. Lett.* **89** 247003
[81] Fauqué B, Sidis Y, Hinkov V, Pailhès S, Lin C T, Chaud X and Bourges P 2006 *Phys. Rev. Lett.* **96** 197001
See also Reznik D, Ismer J-P, Eremin I, Pintschovius L, Arai M, Endoh Y, Masui T and Tajima S 2006 *Preprint* cond-mat/0610755
[82] Shi L, Schmadel D, Drew H D, Tsukada I and Ando Y 2005 *Preprint* cond-mat/0510794
[83] Rast S *et al* 2001 *Phys. Rev.* B **64** 214505
Kusar P, Demsar J, Mihailovic D and Sugai S 2005 *Phys. Rev.* B **72** 014544
Kaindl R A, Carnahan M A, Chemla D S, Oh S and Eckstein J N 2005 *Phys. Rev.* B **72** 060510